

Surface termination effects on the electrical characteristics of La_2O_3/Al_2O_3 nanolaminates deposited by atomic layer deposition

Ji-Bin Fan(樊继斌), Shan-Ya Ling(凌山雅), Hong-Xia Liu(刘红侠), Li Duan(段理), Yan Zhang(张研), Ting-Ting Guo(郭婷婷), Xing Wei(魏星), Qing He(何清)

Citation: Chin. Phys. B . 2020, 29(11): 117701 . **doi:** 10.1088/1674-1056/abc0d4
Journal homepage: http://cpb.iphy.ac.cn; http://iopscience.iop.org/cpb

What follows is a list of articles you may be interested in

Influences of different oxidants on characteristics of La_2O_3/Al_2O_3 nanolaminates deposited by atomic layer deposition

Ji-Bin Fan(樊继斌), Hong-Xia Liu(刘红侠), Li Duan(段理), Yan Zhang(张研), Xiao-Chen Yu(于晓晨)
Chin. Phys. B . 2017, 26(6): 067701 . **doi:** 10.1088/1674-1056/26/6/067701

Performance and reliability improvement of La_2O_3/Al_2O_3 nanolaminates using ultraviolet ozone post treatment

Ji-Bin Fan(樊继斌), Hong-Xia Liu(刘红侠), Bin Sun(孙斌), Li Duan(段理), Xiao-Chen Yu(于晓晨)
Chin. Phys. B . 2017, 26(5): 057702 . **doi:** 10.1088/1674-1056/26/5/057702

Performance improvement of charge trap flash memory by using a composition-modulated high-*k* trapping layer

Tang Zhen-Jie, Li Rong, Yin Jiang
Chin. Phys. B . 2013, 22(9): 097701 . **doi:** 10.1088/1674-1056/22/9/097701

The charge storage characteristics of ZrO_2 nanocrystallite-based charge trap nonvolatile memory

Tang Zhen-Jie, Li Rong, Yin Jiang
Chin. Phys. B . 2013, 22(6): 067702 . **doi:** 10.1088/1674-1056/22/6/067702

Influences of different oxidants on the characteristics of $HfAlO_x$ films deposited by atomic layer deposition

Fan Ji-Bin, Liu Hong-Xia, Ma Fei, Zhuo Qing-Qing, Hao Yue
Chin. Phys. B . 2013, 22(2): 027702 . **doi:** 10.1088/1674-1056/22/2/027702

Surface termination effects on the electrical characteristics of La_2O_3/Al_2O_3 nanolaminates deposited by atomic layer deposition*

Ji-Bin Fan(樊继斌)[1,†], Shan-Ya Ling(凌山雅)[1], Hong-Xia Liu(刘红侠)[2], Li Duan(段理)[1], Yan Zhang(张研)[1], Ting-Ting Guo(郭婷婷)[1], Xing Wei(魏星)[1], and Qing He(何清)[1]

[1] *School of Materials Science and Engineering, Chang'an University, Xi'an* 710061, *China*

[2] *School of Microelectronics, Key Laboratory of Wide Band-Gap Semiconductor Materials and Devices, Xidian University, Xi'an* 710071, *China*

(Received 14 May 2020; revised manuscript received 24 September 2020; accepted manuscript online 14 October 2020)

Effects of initial surface termination on electrical characteristics of La_2O_3/Al_2O_3 nanolaminates deposited by atomic layer deposition are studied by conductive atomic force microscopy working in contact mode and standard electrical characterization methods. It is found that, compared with La_2O_3/Al_2O_3 nanolaminates with LaO_x as termination, lower interface trap density, less current leakage spots, and higher breakdown voltage are obtained in the La_2O_3/Al_2O_3 nanolaminates with AlO_x as termination after annealing. A clear promotion of interface silicate layer is observed for La_2O_3/Al_2O_3 nanolaminates with AlO_x as termination compared with LaO_x as termination under the same annealing condition. In addition, the current conduction mechanism in La_2O_3/Al_2O_3 nanolaminates is considered as the Poole–Frenkel conduction. All results indicate that the AlO_x is a more appropriate termination to deposit La_2O_3/Al_2O_3 nanolaminates on Si substrate, which is useful for the high-κ process development.

Keywords: La_2O_3/Al_2O_3, atomic layer deposition, termination, annealing

PACS: 77.55.D–, 82.80.Pv **DOI:** 10.1088/1674-1056/abc0d4

1. Introduction

High-κ materials have been extensively used to substitute traditional SiO_2 gate dielectrics in sub-22 nm metal-gate complementary metal oxide semiconductor (CMOS) technologies.[1] To realize further improvements in leakage current and power consumption of the CMOS, La-based binary or ternary high-κ materials have been studied by many researchers due to the high dielectric constants, large bandgap, suitable band offset, and good thermal stability when in contact with novel channel materials.[2–4] The accompanying problem of moisture absorption also draws great attention, which can be greatly improved by La_2O_3 mixed with a less hygroscopic oxide Al_2O_3.[5,6] Compared to the layer-by-layer structured film, the nanolaminate processed nanoscale film deposited by atomic layer deposition (ALD) exhibited a high packing density and thermodynamic stability.[7] It can remedy the drawbacks of the individual layers and particularly provide excellent dielectric properties suitable for use in high-performance transistors.[8] However, during the first few cycles of the ALD process, an incomplete reaction of the metal precursor molecules takes place inevitably and the functional groups at the silicon surface are not optimal for adsorption of the metal precursor molecules, generating structural defects and dangling bonds at the interface.[9,10] Improving the properties of the interface between high-κ materials and the substrate has become an important issue for the successful inclusion of high-κ dielectrics in electron devices.

For La_2O_3/Al_2O_3 nanolaminates deposited by ALD on Si substrate, two different surface terminations may appear, LaO_x termination and AlO_x termination. Different surface terminations may affect the construction of the interface layer and the defects at the interface,[11] which affect the electrical characteristics of La_2O_3/Al_2O_3 nanolaminates as the scaling down of semiconductor devices has rapidly progressed. However, to date, this topic has not been systematically studied. Therefore, in this paper, La_2O_3/Al_2O_3 nanolaminates with different terminations are deposited by the ALD. A 1-min thermal annealing is performed in N_2 at 600 °C after deposition, which is compatible with the gate-last CMOS process.[12] Then, a further investigation is carried out to study the surface termination effects on the electrical characteristics of La_2O_3/Al_2O_3 nanolaminates.

2. Experiment

Prior to the deposition, P-type Si(100) wafers with a resistivity of 8–12 Ω·cm are RCA (radio corporation of America) cleaned and then dip in diluted HF for 30 s to remove the native oxide. Tris(isopropylcyclopentadienyl) lanthanum[$La(^iPrCp)_3$] and trimethylaluminum (TMA) are used as precursors of lanthanum and aluminum. Ozone (O_3)

*Project supported by the National Natural Science Foundation of China (Grant Nos. 61604016 and 51802025), China Postdoctoral Science Foundation (Grant No. 2017M613028), the Fundamental Research Funds for the Central Universities, China (Grant Nos. 300102319209 and 300102310501) and the Innovation, and Entrepreneurship Training Program for Undergraduates (Grant Nos. 202010710231 and 201910710564).

†Corresponding author. E-mail: jbfan@chd.edu.cn

© 2020 Chinese Physical Society and IOP Publishing Ltd

is used as the oxidant, which is generated by the ozone generator using ultra-pure O_2 (99.999%). A LaO_x (or AlO_x) surface termination is firstly formed on the Si substrates by 5 ALD cycles, and then the same processed 10 ALD cycles of La_2O_3/Al_2O_3 nanolaminates are grown using metal processors ($La(^iPrCp)_3$, TMA) and O_3 at the growth temperature of 300 °C. The La_2O_3/Al_2O_3 nanolaminates with LaO_x termination and with AlO_x termination is denoted as nanolaminate-LaO_x and nanolaminate-AlO_x, respectively. The structures of the La_2O_3/Al_2O_3 nanolaminates with different terminations were shown in Fig. 1. After the samples annealed in the nitrogen at 600 °C for 60 s, the x-ray photoelectron spectroscopy (XPS, Thermo Scientific K-Alpha), conductive atomic force microscopy (CAFM, Bruker Dimension Edge) measurements are performed to investigate the characteristics of La_2O_3/Al_2O_3 nanolaminates. A metal electrode is fabricated by depositing 200 nm Al using electron beam evaporation, followed by photolithography patterning to form MOS capacitors. After that, the standard electrical measurements are performed at room temperature using Keithley 590 CV meter and Agilent E4980A characterization system.

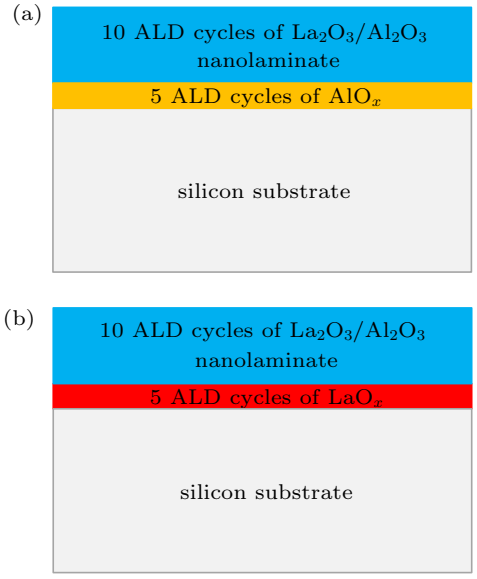


Fig. 1. Structures of the La_2O_3/Al_2O_3 nanolaminates with (a) AlO_x termination, and (b) LaO_x termination.

3. Results and discussion

Figure 2 shows the *C*–*V* curves of La_2O_3/Al_2O_3 nanolaminates with different terminations. The gate voltage (V_G) is first swept from forward (negative to positive) and then backward (positive to negative) at the frequency of 100 kHz. As shown in Fig. 2, the *C*–*V* curve of nanolaminate-AlO_x is shifted positively after annealing, whereas the *C*–*V* curve of nanolaminate-LaO_x is shifted negatively after annealing. The different V_{FB} shift in the *C*–*V* curves can be explained by the dipoles formed differently at the interfacial layer.[13] In addition, the accumulation capacitance values of nanolaminate-LaO_x decreased sharply whereas the accumulation capacitance values of nanolaminate-AlO_x changed negligibly. Densification of the nanolaminate after annealing usually results in an increase in capacitance value.[5] The decrease in the capacitance value may be explained by the formation of the interfacial layer with a low dielectric constant after annealing. Furthermore, a hump is observed at about 0.5 V in the *C*–*V* curve of the as-deposited nanolaminate-AlO_x and it disappears after annealing, whereas that of the as-deposited nanolaminate-LaO_x is not obvious and the negligible hump at about 0 V disappears after annealing. The hump indicates that there many traps in the near interface.[14] After annealing, the hump disappears which can be attributed to the decrease of defects and dangling bonds near the interface during the annealing process.

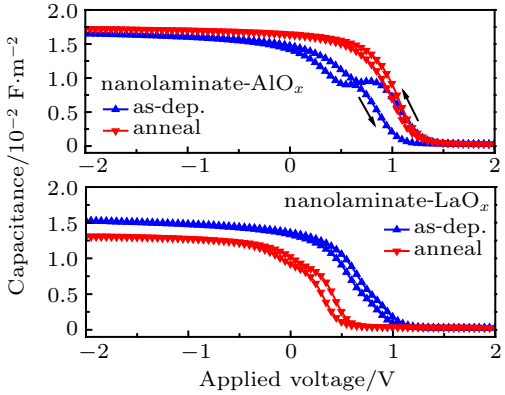


Fig. 2. The *C*–*V* characteristics of La_2O_3/Al_2O_3 nanolaminates with different terminations ($f = 100$ kHz).

For the further accurate evaluation of interfacial properties, the interface trap density, D_{it}, is investigated by using the conductance method. Figure 3 shows the G/ω–f plots of the La_2O_3/Al_2O_3 nanolaminates with different terminations. The D_{it} is deduced from simplified conductance (G_p) which is derived from equivalent circuits.[15] As shown in Fig. 3, the D_{it} value of as-deposited nanolaminate-AlO_x and nanolaminate-LaO_x is 1.698×10^{13} $cm^{-2}\cdot eV^{-1}$ and 1.349×10^{13} $cm^{-2}\cdot eV^{-1}$, respectively. The results indicate that the $\sim 26\%$ increase of the D_{it} is obtained by choosing AlO_x as the termination compared with LaO_x as the termination, which is consistent with the *C*–*V* measurement. Unlike water can generate the hydrogen/hydroxyl sources which will further improve the passivation of silicon during the H_2O-based ALD deposition, ozone as the oxidant will show a higher interface trap density.[16] After annealing, the D_{it} of nanolaminate-AlO_x decreases from 1.698×10^{13} $cm^{-2}\cdot eV^{-1}$ to 8.64×10^{12} $cm^{-2}\cdot eV^{-1}$, whereas the D_{it} value of nanolaminate-LaO_x slightly decreases from 1.349×10^{13} $cm^{-2}\cdot eV^{-1}$ to 1.244×10^{13} $cm^{-2}\cdot eV^{-1}$. This may be explained by, at the beginning of the ALD cycles, the incomplete reaction of the metal pre-

cursor molecules and oxidant generated the defects, the dangling bonds, and unpaired bonding traps in the layer. Thermal annealing supplied enough thermal energy for the traps or defects decomposition and re-composition, the traps or defects decreased after annealing.[4] The interface state density is strongly correlated to the quality of the dielectric, and has been used to characterize gate dielectric reliability.[17] Therefore, compared with LaO_x as the termination, the properties of the interface can be improved by choosing AlO_x as the surface termination because of its lower D_{it} after annealing.

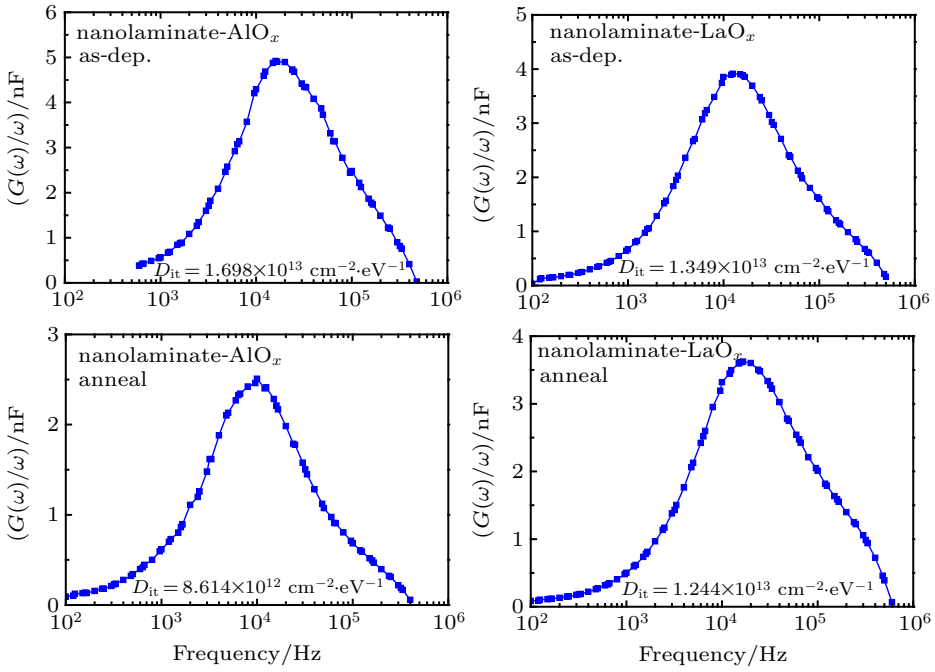


Fig. 3. Interface state density of La_2O_3/Al_2O_3 nanolaminates with different terminations.

Due to conductive AFM able to characterize the gate dielectric on a nanometer/micrometer scale, showing properties to which the standard electrical characterization techniques are blind.[18,19] Figure 4 shows the current images obtained with the CAFM at a conductive tip voltage of 2 V for La_2O_3/ Al_2O_3 nanolaminates with different terminations on Si substrate. The spatial distribution of conductivity for La_2O_3/Al_2O_3 nanolaminates can be derived from the current images. As shown in Figs. 4(a) and 4(b), the density of leakage spot in the as-deposited nanolaminate-AlO_x is very low in a 5 μm×5 μm area and the leakage spots decreases after annealing. For the as-deposited nanolaminate-LaO_x, the density of the leakage spot is smaller compared with the as-deposited nanolaminate-AlO_x. However, the density of leakage spots increases significantly after annealing, as shown in Figs. 4(c) and 4(d). It can be concluded that the conductive paths in the nanolaminate-LaO_x increased significantly after annealing depending on the increase in the number of leakage current spots. It may be caused by the local fluctuations in composition and/or structures, and/or by defects in the nanolaminates which is related to the formation of a low dielectric constant silicate layer.[4,20] The results suggest that La_2O_3/Al_2O_3 nanolaminates with AlO_x termination shows less conductive feature compared to the La_2O_3/Al_2O_3 nanolaminates with LaO_x termination after annealing, which is consistent with the standard electrical characterization methods results.

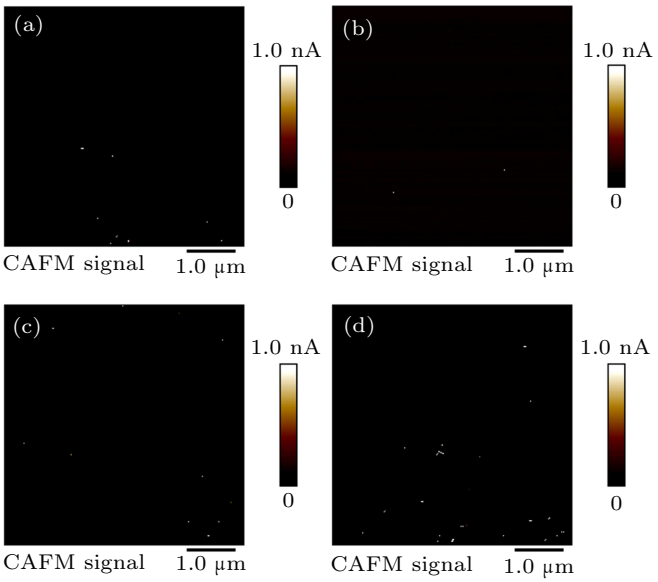


Fig. 4. The CAFM images of (a) as-deposited nanolaminate-AlO_x, (b) annealed nanolaminate-AlO_x, (c) as-deposited nanolaminate-LaO_x, and (d) annealed nanolaminate-LaO_x measured by conductive AFM with a conductive tip.

More detailed information on conduction for La_2O_3/Al_2O_3 nanolaminates with different terminations can be obtained from further data analysis of the *I*–*V* curves measured on fixed locations. Figure 5 shows the *I*–*V* curves of

La_2O_3/Al_2O_3 nanolaminates measured by the CAFM using a Pt-coated tip at the room temperature. As shown in the Fig. 5, The breakdown voltage of the as-deposited nanolaminate-AlO_x is 8.22 V at the leakage current of 1 nA while that of the as-deposited nanolaminate-LaO_x is 7.95 V. After annealing, the breakdown voltage of the nanolaminate-AlO_x increases to 8.41 V and that of nanolaminate-LaO_x decreases to 6.59 V. The decrease of the breakdown voltage for the nanolaminate-LaO_x may be caused by that the formation of the interfacial layer leads to the deterioration of interface and nanolaminates.[21]

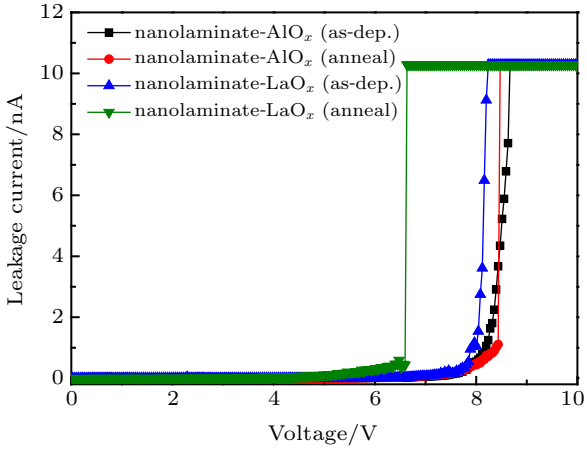


Fig. 5. The *I–V* curves of the La_2O_3/Al_2O_3 nanolaminates measured at the positions of conductive spots in the CAFM images.

The leakage current is governed by the emission of electrons via trap state into a continuum of states associated with the presence of conductive dislocations.[22] The forward *I–V* curves have been analyzed in terms of various conduction mechanisms to find that the data can be fitted best to the Frenkel–Poole mechanism.[19] The current density associated with the Frenkel–Poole mechanism is given by[23]

$$J = AE \times \exp\left(-\frac{q\phi_t}{kT} + \frac{\sqrt{q^3E/\pi\varepsilon_0\varepsilon_s}}{kT}\right), \qquad (1)$$

where J, q, E, T, ϕ_t, A, k, ε_0, and ε_s are the current density, the electron charge, the electric field over the energy barrier at the tip-semiconductor interface, the absolute temperature, the barrier height for electron emission from the trapped state, a constant, the Boltzmann constant, the vacuum dielectric permittivity, and the relative dielectric permittivity of the semiconductor, respectively. Figure 6 shows the plot of $\ln(J/E)$ as a function of $E^{1/2}$ obtained from the *I–V* curves of Fig. 5. As shown in Fig. 6, the plot of $\ln(J/E)$ as a function of $E^{1/2}$ follows a trend of the linear relationship. It suggests that the conduction through La_2O_3/Al_2O_3 nanolaminates with different terminations is consistent with the Frenkel–Poole mechanism.

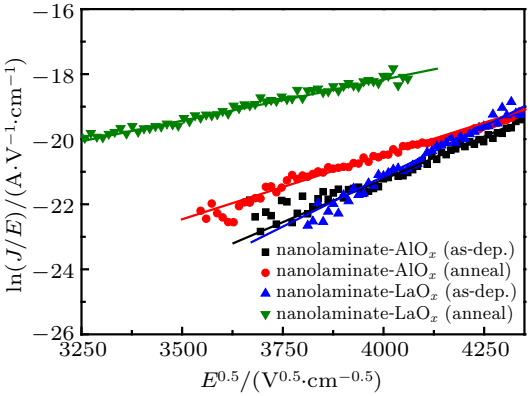


Fig. 6. The plot of $\ln(J/E)$ versus $E^{1/2}$ obtained from the *I–V* curves of Fig. 5.

To further confirm the changes in the electrical properties of La_2O_3/Al_2O_3 nanolaminates after annealing due to the different surface terminations, figure 7 shows the O_{1s} XPS spectra of La_2O_3/Al_2O_3 nanolaminates with different terminations. The C_{1s} peak from adventitious carbon at 284.80 eV is used as an internal energy reference to correct the differential charging during the analysis. As shown in Fig. 7, for the nanolaminate-AlO_x, the O_{1s} core level spectrum consists of four fitting peaks. Three fitting peaks located at a binding energy of 529.40 eV, 530.32 eV, and 531.12 eV, can originate from La–O–La, La–O–Al, and Al–O–Al, respectively.[24,25] The remaining peak located at 532.18 eV is indicative of a silicate formation.[26] According to the fitting peak intensity and surface termination, an ultra-thin aluminum silicate-like layer should be formed at the interface between the nanolaminate and Si. After annealing, the peak intensity of silicate increases slightly. For the nanolaminate-LaO_x, the O_{1s} core level spectrum also consists of four fitting peaks. Three fitting peaks located at a binding energy of 529.49 eV, 530.42 eV, and 531.27 eV, can originate from La–O–La, La–O–Al, and Al–O–Al, respectively.[24,25] The remaining peak located at 532.38 eV is indicative of an ultra-thin lanthanum silicate formation.[26] After annealing, the peak intensity of silicate increases significantly, which indicates a large amount of interfacial silicate formation caused by the intermixing of Si and La atoms. The formation of La–O–Si can be explained by the more favorable free energy compared with that of La–O–Al, Al–O–Si, La–O, or Si–O.[27] The result indicates that the interface of the aluminum silicate layer serves as a diffusion barrier to suppress the diffusion of Si and other atoms, whereas lanthanum silicate cannot serve as a diffusion barrier at the annealing temperature. Therefore, the electrical properties of La_2O_3/Al_2O_3 nanolaminates with different terminations change differently after annealing due to the different interface formation.

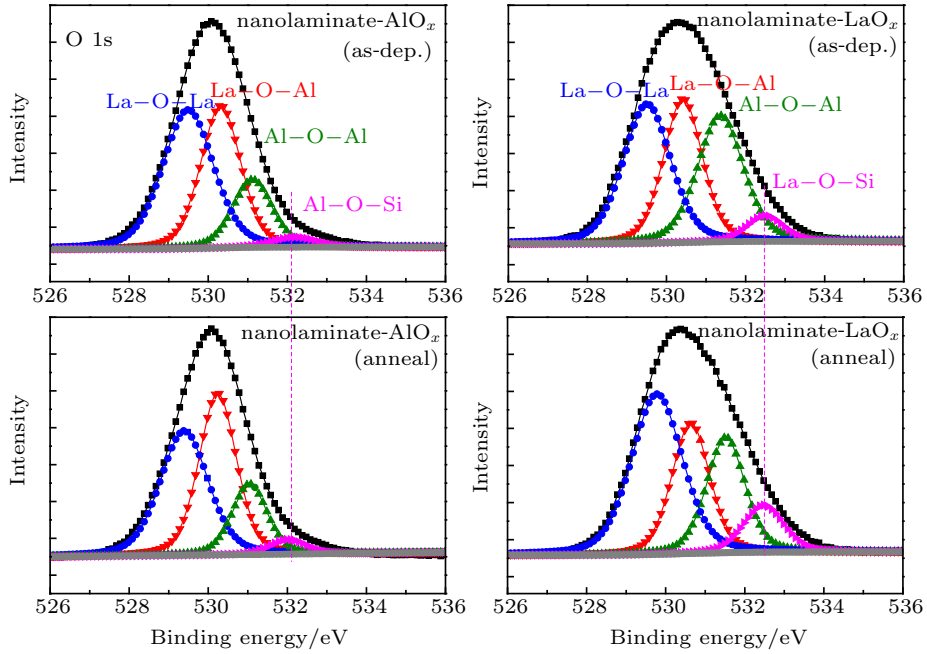


Fig. 7. The O_{1s} spectra of La_2O_3/Al_2O_3 nanolaminates with different terminations deposited by the ALD.

4. Conclusions

Surface termination effects on the electrical characteristics of La_2O_3/Al_2O_3 nanolaminates are investigated after annealing. It is found that with the help of the standard electrical characterization methods, La_2O_3/Al_2O_3 nanolaminates with AlO_x as termination shows lower interface state density and better *C*–*V* characteristics after annealing compared with LaO_x as termination. The conductive AFM results indicate that compared to the La_2O_3/Al_2O_3 nanolaminates with LaO_x termination, La_2O_3/Al_2O_3 nanolaminates with AlO_x termination present less conductive spots and higher breakdown voltage after annealing. The current conduction mechanism in La_2O_3/Al_2O_3 nanolaminates is considered the Poole–Frenkel conduction. The XPS results show that a clear improvement in the interface silicate layer is observed for La_2O_3/Al_2O_3 nanolaminates with AlO_x as termination compared with LaO_x as termination at the same annealing condition. All results indicate that AlO_x is a more appropriate termination to deposit La_2O_3/Al_2O_3 nanolaminates for electron devices application.

References

[1] Gupta S, Gong X, Zhang R, Yeo Y C, Takagi S and Saraswat K C 2014 *MRS Bull.* **39** 678

[2] Ablat A, Mamat M, Ghupur Y, Aimidula A, Wu R, Ali Baqi M, Gholama T, Wang J, Qian H, Wu R and Ibrahim W 2017 *Mater. Lett.* **191** 97

[3] Mcdaniel M D, Ngo T Q, Hu S, Posadas A, Demkov A A and Ekerdt J G 2015 *Appl. Phys. Rev.* **2** 041301

[4] Fan J B, Liu H X, Li D L, Wang S L, Duan L and Yu X C 2017 *J. Mater. Sci.: Mater. Electron.* **28** 11253

[5] Fujitsuka R, Sakashita M, Sakai A, Ogawa M and Yasuda Y 2005 *Jpn. J. Appl. Phys.* **44** 2428

[6] Fei C X, Liu H X, Wang X, Zhao D D, Wang S L and Chen S P 2016 *Chin. Phys. B* **25** 058106

[7] Baek Y, Lim S, Kim L H, Park S, Lee S W, Oh T H, Kim S H and Park C E 2015 *Org. Electron.* **28** 139

[8] Kim L H, Kim K, Park S, Jeong Y J, Kim H, Chung D S, Kim S H and Park CE 2014 *ACS Appl. Mater. Interfaces* **6** 6731

[9] Werner F, Veith B, Zielke D, Kühnemund L, Tegenkamp C, Seibt Michael, Brendel1 R and Schmidt J 2011 *J. Appl. Phys.* **109** 113701

[10] Goncharova L V, Dalponte M, Feng T, Gustafsson T, Garfunkel E, Lysaght P S and Bersuker G 2011 *Phys. Rev. B* **83** 115329

[11] Travis C D and Adomaitis R A 2013 *Chem. Vap. Deposition* **19** 4

[12] Mistry K, Allen C, Auth C, Beattie B, Bergstrom D, BostM, BrazierM, BuehlerM, Cappellani A, Chau R, Choi C H, Ding G, Fischer K, Ghani T, Grover R, Han W, Hanken D, Hattendorf M, He J and Zawadzki K 2007 *Int. Electron Devices Meet.* 247

[13] Iwamoto K, Kamimuta Y, Ogawa A, Iwamoto K, Kamimuta Y, Ogawa Arito, Watanabe Y, Migita S, Mizubayashi W, Morita Y, Takahashi M, Ota H, Nabatame T and Toriumi A 2008 *Appl. Phys. Lett.* **92** 132907

[14] Min K H, Choi S, Jeong M S, Kang M G, Park S, Song H E, Lee J I and Kim D W 2019 *Curr. Appl. Phys.* **19** 155

[15] Matsuoka R, Shigesawa E, Miyamoto S, Sawano K and Itoh K M 2019 *Semicond. Sci. Tech.* **34** 014004

[16] Von Gastrow G, Li S, Repo P, Bao Y, Putkonen M and Savin H 2013 *Energy Procedia* **38** 890

[17] Vogel E M, Henson W K, Richter C A and Suehle J S 2000 *IEEE T. Electron. Dev.* **47** 601

[18] Iglesias V, Wu Q, Porti M, Nafría M, Bersuker G, Cordes A 2015 *Microelectron. Eng.* **147** 31

[19] Fan J B, Cheng X J, Liu H X, Wang S L and Duan L 2017 *Chin. Phys. B* **26** 087701

[20] Molina J, Tachi K, Kakushima K, Ahmet P and Hiroshi I 2006 *ECS Trans.* **3** 233

[21] Eom D, Hwang C S, Kim H J, Cho M H and Chung K B 2008 *Electrochem. Solid-State Lett.* **11** G33

[22] Couso C, Iglesias V, Porti M, Claramunt S, Nafria M, Domingo N, Cordes A and Bersuker G 2016 *IEEE Electron Dev. Lett.* **37** 640

[23] Rao P K, Park B, Lee S T, Noh Y K, Kim M D and Oh J E 2011 *J. Appl. Phys.* **110** 013716

[24] Besmehn A, Scholl A, Rije E and Breuer U 2005 *Appl. Surf. Sci.* **252** 172

[25] Guittet M J, Crocombette J P and Gautier-Soyer M 2001 *Phys. Rev. B* **63** 125117

[26] Lin L I, Tang Z, Sun W and Wang P 1999 *J. Mater. Sci. Tech.* **15** 439

[27] Lee B, Novak S R, Lichtenwalner D J, Yang X and Misra V 2011 *IEEE T. Electron. Dev.* **58** 3106